Fabrication and Characterization of Advanced Triple-junction Amorphous Silicon Based Solar Cells

PHASE II – Quarter 4

Quarterly Technical Progress Report

December 1, 2006 to February 28, 2007

NREL Subcontract No. ZXL-5-44205-06

Subcontractor: The University of Toledo

Principal Investigator: Xunming Deng
(419) 530-4782; dengx@physics.utoledo.edu

Co-Principal Investigator: Robert W. Collins
(419) 530-2195; rcollins@physics.utoledo.edu

Department of Physics and Astronomy
University of Toledo, Toledo, OH 43606

Contract technical monitor: Dr. Bolko von Roedern

Table of Contents

Section 1

Executive Summary

This quarterly technical progress report covers the highlights of the research activities and results on the project of "The Fabrication and Characterization of High-efficiency Triple-junction a-Si Based Solar Cells" at the University of Toledo for the Period of December 1, 2006 to February 28, 2007, under NREL TFPPP subcontract number ZXL-5-44205-06.

Following this Executive Summary are the sections performed during this quarter related to the tasks under this subcontract. The major technical progresses of these sections are summarized as follows:

Section 2: Application of Real Time Spectroscopic Ellipsometry to the Analysis of Compositionally Graded a-$Si_{1-x}Ge_x$:H Thin Films

We have applied an advanced analytical model to analyze the dielectric functions $\varepsilon = \varepsilon_1 + i\varepsilon_2$ of amorphous silicon-germanium alloys (a-$Si_{1-x}Ge_x$:H) versus alloy content x by varying the flow ratio G = $[GeH_4]/\{[SiH_4]+[GeH_4]\}$ in plasma-enhanced chemical vapor deposition (PECVD). All spectra (1.5 – 4.5 eV) have been measured accurately by spectroscopic ellipsometry (SE) either in real time during deposition or in situ post-deposition in order to quantify and eliminate surface roughness effects and also to avoid surface contamination. From the resulting extensive database, the optical properties of the alloys can be predicted for any value x and temperature of measurement T_m within the ranges covered by the database. Such a database has been used in the analysis of a-$Si_{1-x}Ge_x$:H thin films prepared by varying the flow ratio G as a function of time within a single deposition. The analysis of the resulting film uses not only the database but also the virtual interface analysis approach in order to extract the time evolution of the instantaneous deposition rate r(t) and the germanium content x(t) in the outerlayer (top-most ~ 7 Å) of the bulk film. In addition, the evolution of the surface roughness thickness $d_s(t)$ is extracted. From r(t) and x(t), a depth profile in the alloy content $x(d_b)$ is obtained where the independent variable d_b describes the bulk layer thickness (or depth from the substrate interface).

Section 3: ZnO film thickness study for Ag/ZnO back reflector

ZnO film as a buffer layer between the metal back reflector (BR) and the amorphous or nano-crystalline silicon layers is a standard structure in thin film silicon solar cells. It is desirable to have certain thickness to prevent the inter-diffusion of metal and silicon. It may need even thicker ZnO layer to fully cover the metal surface when the metal layer is highly textured. But the thicker ZnO layer may absorb much light and cause extra optical loss. This work is trying to study the optical losses of ZnO films for BR usage. A series of intrinsic ZnO films was prepared using RF magnetron-sputtering technique. The as-deposited ZnO films has very good transmittance. The integrated optical absorption loss on solar spectrum over range 600 ~ 1200 nm is only about 2.54% with a thickness about 2300 nm. When the complete Ag/ZnO BRs are evaluated by nc-Si cells on glass, it shows that the thicker ZnO leads to smaller J_{sc}. But this

method needs further analysis since there is an air gap which may cause extra optical loss during measuring.

Section 4: Optical Simulations of the Effects of Ag/ZnO Interlayer at the Back-Reflector for Thin Film a-Si:H Solar Cells

Optical simulations have been performed to investigate the effect of Ag/ZnO interface layers in back-reflectors for thin film triple junction a-Si:H solar cells in the n-i-p configuration. The role of interface layers generated by differing amounts of initial Ag surface roughness has been explored. It has been observed that increasing the initial surface roughness of Ag increases the losses through absorption in the interlayer. As expected, increasing the interface thickness for a given interface layer dielectric function enhances the absorption losses in the interlayer. The goal of the back-reflector fabrication studies is to identify the origins of the interface losses and eliminate them through modifications in the back-reflector design. Modeling studies such as these supplement the experimental work and predict the improvements that may be expected.

Section 2

Application of Real Time Spectroscopic Ellipsometry to the Analysis of Compositionally Graded a-$Si_{1-x}Ge_x$:H Thin Films

N. J. Podraza and R. W. Collins

Department of Physics and Astronomy, University of Toledo, Toledo, OH 43606

1. Introduction and Overview

We have applied an advanced analytical model to analyze the dielectric functions $\varepsilon = \varepsilon_1 + i\varepsilon_2$ of amorphous silicon-germanium alloys (a-$Si_{1-x}Ge_x$:H) versus alloy content x by varying the flow ratio $G = [GeH_4]/\{[SiH_4]+[GeH_4]\}$ in plasma-enhanced chemical vapor deposition (PECVD). All ε spectra (1.5 – 4.5 eV) have been measured accurately by spectroscopic ellipsometry (SE) either in real time during deposition or in situ post-deposition in order to quantify and eliminate surface roughness effects and also to avoid surface contamination. From the resulting extensive database, the optical properties of the alloys can be predicted for any value x and temperature of measurement T_m within the ranges covered by the database. Such a database has been used in the analysis of a-$Si_{1-x}Ge_x$:H thin films prepared by varying the flow ratio G as a function of time within a single deposition. The analysis of the resulting film uses not only the database but also the virtual interface analysis approach in order to extract the time evolution of the instantaneous deposition rate r(t) and the germanium content x(t) in the outerlayer (top-most ~ 7 Å) of the bulk film. In addition, the evolution of the surface roughness thickness $d_s(t)$ is extracted. From r(t) and x(t), a depth profile in the alloy content $x(d_b)$ is obtained where the independent variable d_b describes the bulk layer thickness (or depth from the substrate interface).

2. Experimental Details: Deposition Processes

The a-$Si_{1-x}Ge_x$:H films were deposited using single-chamber rf (13.56 MHz) plasma enhanced chemical vapor deposition (PECVD) and were measured in real time using a rotating-compensator multichannel ellipsometer. The substrates were native-oxide/c-Si mounted on the cathode (self bias $V_{dc} \sim -20$ V) of the reactor. The PECVD conditions adopted here include a relatively low substrate temperature (T = 200°C; actual surface value calibrated by SE), the minimum plasma power possible for a stable plasma (0.08 mW/cm^2), a low partial pressure of the source gases $\{[SiH_4]+[GeH_4]\}$ (~ 0.06 Torr), a total pressure of less than 1.0 Torr, and a H_2-dilution level of $R = [H_2] / \{[SiH_4] + [GeH_4]\} = 10$. The GeH_4 flow ratio $G = [GeH_4]/\{[SiH_4]+[GeH_4]\}$ was varied over the range $0 \leq G \leq 0.167$ for a series of five individual depositions in order to tabulate a set of reference dielectric functions, $\varepsilon = \varepsilon_1 + i\varepsilon_2$. For a single graded layer deposition described in detail here as a example, G was varied as a function of time in a stepwise fashion from G = 0.042 to G = 0.15 and then to G = 0 to produce a structure with a compositionally graded Ge content, x, as can be used in a solar cell device with a graded bandgap structure [1,2].

For the series of individual depositions, Fig. 1 shows the variation in x (left scale) and a measure of the optical band gap E_g (right scale) both as functions of G. Because of the close linearity between E_g and x, the left and right scales in Fig. 1 can be chosen so that the data points coincide within the error bars. The composition x is obtained ex situ by x-ray photoelectron spectroscopy, and E_g is obtained from real time SE, applying an extrapolation of $\varepsilon_2^{1/2}$ versus photon energy E, assuming parabolic bands and a constant-dipole matrix element (CD-ME, method of G. Cody) [3]. It should be noted that the T = 200°C gap of 1.17 eV at G=0.167 in Fig. 1 corresponds to a T = 20°C Tauc gap of 1.28 eV. The Tauc method is based on the assumptions of parabolic bands and a constant-momentum matrix element (CM-ME).

3. Experimental Details: Optical Model

The most popular full dielectric function parameterization for amorphous semiconductors is based on a model for ε_2 that includes a parabolic-band, CM-ME expression $G_M(E)=(E-E_g)^2/E^2$ at near gap energies, evolving to a Lorentz oscillator $L(E) = AE_0\Gamma E/[(E_0^2-E^2)^2 + \Gamma^2E^2]$ at high energies, including a total of four free parameters $\{E_g, A, E_0, \Gamma\}$ [4]. Then ε_1 is given by an analytical Kramers-Kronig integration of $\varepsilon_2(E)=G_M(E)L(E)$; $E>E_g$ and $\varepsilon_2=0$; $E<E_g$. In fact, in determining ε_1, a fifth free parameter is introduced, the constant contribution to the dielectric function ε_∞. More recent research has shown that a similar approach that adopts instead a CD-ME formalism $G_D(E) = (E-E_g)^2/[(E-E_g)^2+E_p^2]$ at near gap energies provides a superior fit with improved internal consistency [3]. Thus, in order to couple the CD-ME expression to the Lorentz oscillator, the additional parameter E_p is required that controls the transition energy

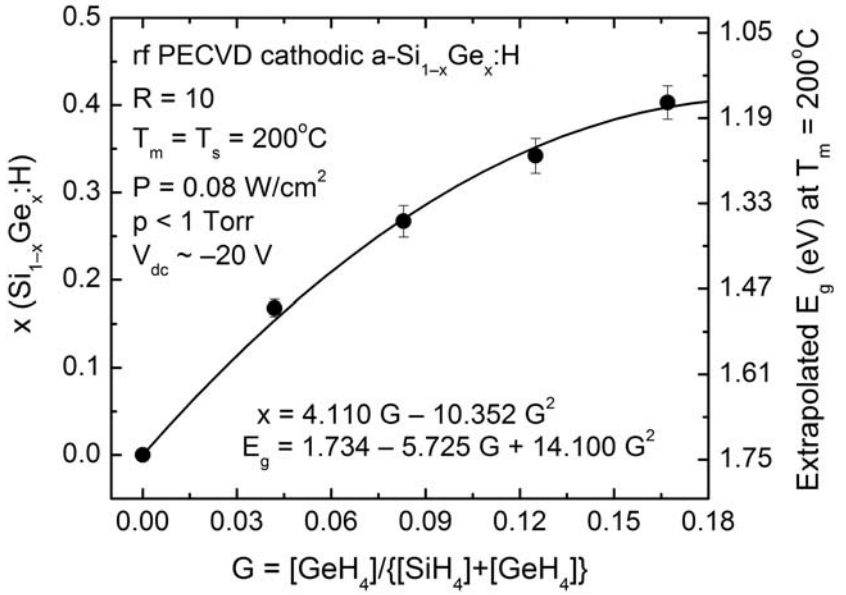

Fig. 1 The alloy content x in a-$Si_{1-x}Ge_x$:H thin films (left scale) and their optical band gaps at T = 200°C (right scale) as functions of the flow ratio G = $[GeH_4]/\{[SiH_4] + [GeH_4]\}$, using a fixed ratio R=$[H_2]/\{[SiH_4] + [GeH_4]\}$=10 and a cathodic electrode configuration. The gaps are from extrapolations of $\varepsilon_2^{1/2}$ to zero ordinate using ε_2 obtained by inversion at thicknesses in the range of 150-300 Å. Because of the linearity in E_g vs. x, the data points coincide within the error bars.

between the near gap absorption onset and the Lorentz oscillator behavior. The extra parameter of the CD-ME approach is compensated through improved consistency that allows fixing $\varepsilon_\infty = 1$. In contrast, for the CM-ME, ε_∞ decreases with increasing x, becoming negative for the larger values of x, unphysical behavior [3]. Fig. 2 shows examples of the experimental data and fits to the CD-ME approach for cathodic a-$Si_{1-x}Ge_x$:H prepared with R=10 and with the extremes of G=0 and 0.167.

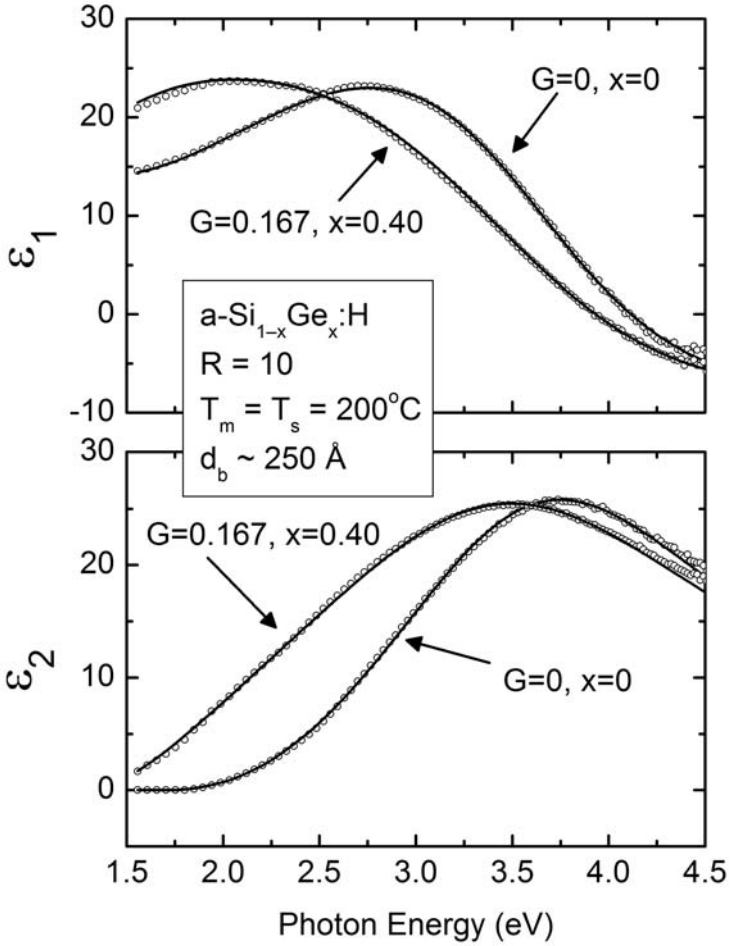

Fig. 2 Examples of fits (solid lines) to dielectric function spectra measured at T = 200°C (points) for a-$Si_{1-x}Ge_x$:H films from the series of Fig. 1 (R=10, cathodic deposition) at the extremes of the alloy range. These spectra were deduced by inversion of real time SE data at bulk layer thicknesses in the range 150-300 Å.

4. Results and Discussion

Figure 3 depicts data (solid points) in the best fit variable parameters of the CD-ME formula plotted versus x. In the formula, ε_∞ is fixed at 1. In addition, the resonance energy E_0 is found to be constant at 3.736 eV within the confidence limits, and so is also fixed. The samples analyzed to obtain the results in Fig. 3 were from the deposition series using the cathodic configuration with R fixed at 10. The results are characteristic of T = 200°C and also a film thickness of ~150 - 300 Å. The variations with x of interest

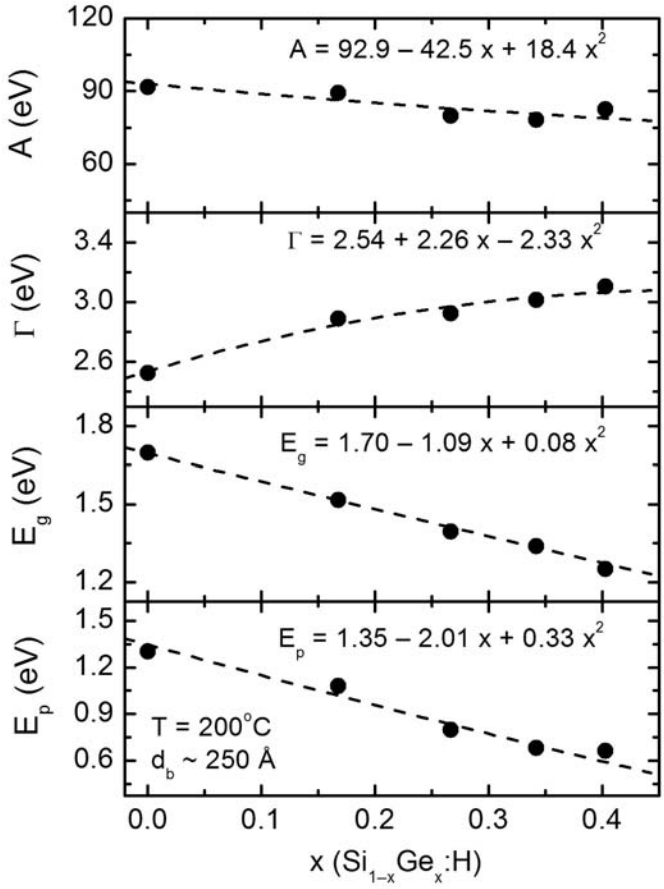

Fig. 3 (left) Dielectric function parameters at T = 200°C plotted versus a-$Si_{1-x}Ge_x$:H alloy composition x. These parameters were deduced in fits such as those of Fig. 2 for the series of depositions of Fig. 1. The dielectric functions fitted in this study were obtained by inversion at bulk layer thicknesses of ~ 150-300 Å. The following parameters were fixed in the analysis: $\varepsilon_\infty = 1$ and $E_0 = 3.736$ eV.

include the expected, nearly linear decreases in the fitted E_g (distinct from the $\varepsilon_2^{1/2}$ extrapolation for E_g in Fig. 1) and transition energy E_p. Of equal interest is the monotonic increase in the width parameter Γ. This is attributed to a reduction in the excited state lifetime due to increased disorder with alloying. In fact, assuming electron and hole velocities υ characteristic of the E_1 excited states of c-Si and using the simple expression for the mean free path $L = h\upsilon/\Gamma$ (h: Planck's constant), a 2 → 3 eV dielectric function width can be ascribed to a 5 → 4 Å mean free path, which is consistent with the lack of long-range ordering. Thus, the width Γ is a very useful parameter for assessing short-range order, also found to correlate with the Urbach tail width [3]. In fact, its usefulness lies in its accessibility in a real time measurement. Finally, the parameterization of the dielectric functions from this series of films and the consistent dependence of the parameters on Ge content x allow us to generate the dielectric function for a-$Si_{1-x}Ge_x$:H prepared under these conditions for any value x from 0 to 0.40.

A four medium [ambient / (surface roughness layer) / (bulk outerlayer) / pseudosubstrate] virtual interface approximation has been used to analyze compositionally graded a-$Si_{1-x}Ge_x$:H films in order to extract the surface roughness thickness evolution, instantaneous deposition rate, and Ge content x in the outer bulk layer (or "outerlayer") as a function of time [5]. It is important to note that x is used as a single parameter to describe the dielectric function of the outerlayer, as based on the relationships described between the Cody-Lorentz parameters and the Ge content described above. Figure 4 shows representative results of such an analysis including (a) the flow ratio G, which controls the compositional profile; (b) the surface roughness layer thickness d_s; (c) the instantaneous growth rate r determined from the virtual interface analysis (circles) and predicted from a theoretical calculation based on G(t), assuming instantaneous response (solid line); and (d) the Ge content x in the outerlayer (top ~7 Å)

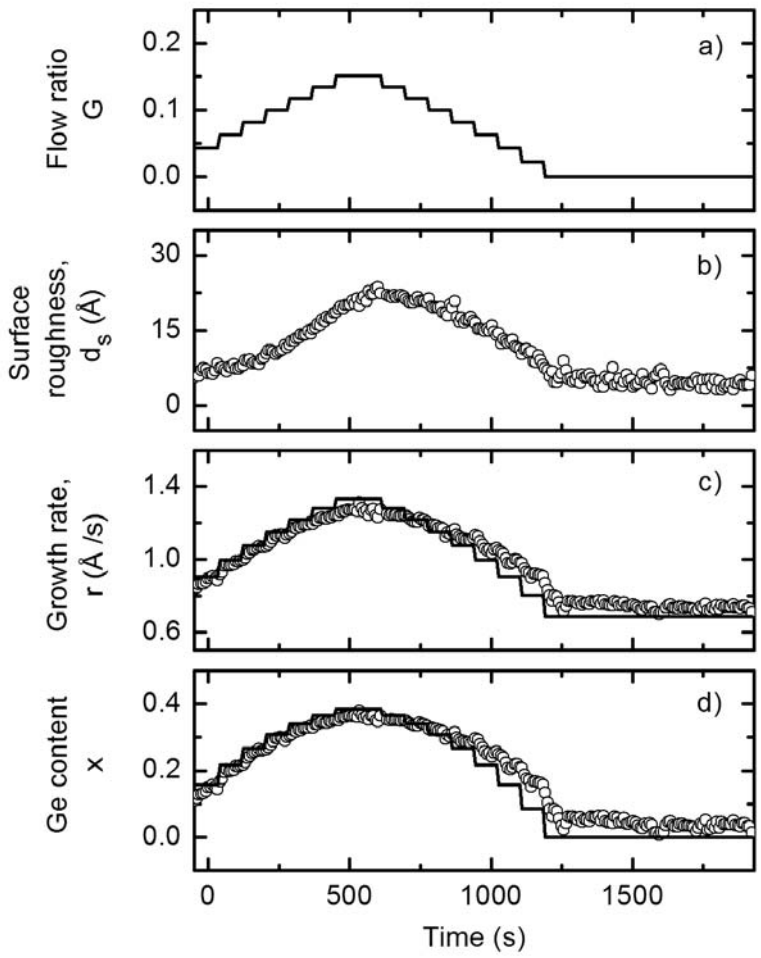

Fig. 4 Time evolution of (a) flow ratio G = $[GeH_4]$ / {$[SiH_4]$+$[GeH_4]$} varied in a step-wise fashion for a multilayer alloy structure (G = 0.042 → 0.15 → 0), (b) the surface roughness layer thickness, (c) the instantaneous deposition rate, and (d) the Ge content of the topmost ~ 7 Å of the bulk layer (or "outerlayer"), all for an a-$Si_{1-x}Ge_x$:H film prepared on a G = 0.042, R = 10 a-$Si_{1-x}Ge_x$:H substrate. The open circles represent experimental data obtained from a virtual interface analysis that interprets the film as a graded layer, while the solid lines represent predicted results based on the value of G and the series of individual depositions.

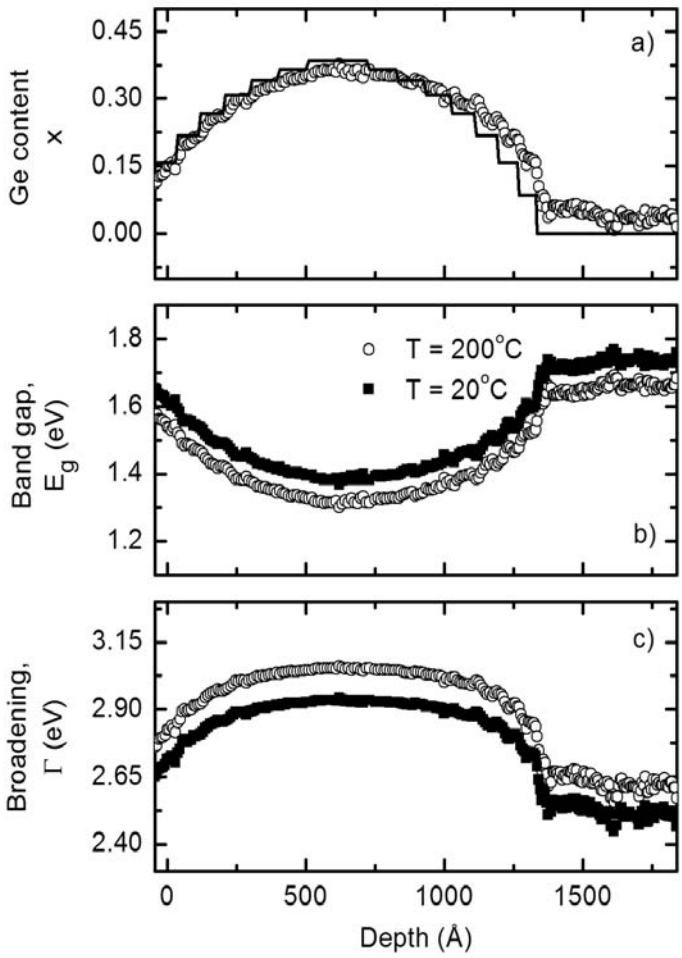

Fig. 5 Depth profiles for the multilayer structure (G = 0.042 → 0.15 → 0) in (a) Ge content from virtual interface analysis (open circles) and theoretical prediction (solid line) assuming instantaneous response to the flow ratio G, (b) band gap E_g at the deposition temperature T = 200°C and at room temperature T = 20°C, and (c) dielectric function broadening Γ at the deposition temperature T = 200°C and at room temperature T = 20°C.

as determined from virtual interface analysis (circles) and from a theoretical calculation based on G(t) (solid line), again assuming instantaneous response. It is apparent from Fig. 4 that the GeH_4 present in the deposition process does not immediately respond to decreases in the flow ratio G, due to a long residence time in the chamber, resulting in the disappearance of a clear stepwise structure in favor of a more gradual decrease in Ge content over a period of time. Finally, Fig. 5 depicts (a) the Ge content x; (b) the bandgap E_g at T = 200°C (circles) and T = 20°C (squares); and (c) the dielectric function broadening Γ at T = 200°C (circles) and T = 20°C (squares) all as a function of a depth from the substrate interface obtained from Fig. 4 by integration of the instantaneous growth rate with respect to time. The dielectric function characteristics E_g and Γ at T = 200°C were extracted from x via the parameterizations in Fig. 3 and the appropriate temperature dependence [6] was used to extract their values at T = 20°C.

5. Summary

In this work we have established a database of a-$Si_{1-x}Ge_x$:H dielectric function spectra as a function of Ge content x. This dielectric function database was then applied to the analysis of a compositionally graded a-$Si_{1-x}Ge_x$:H thin film, where a four medium virtual interface analysis was used to extract the surface roughness evolution, instantaneous growth rate, and Ge content x as functions of time or alternatively as functions of bulk layer thickness (or depth from the substrate interface). The relationships between x and the various Cody-Lorentz energy-independent dielectric function parameters also make it possible to extract any of those parameters as functions of time or depth once the value of x is known. The ability of real time spectroscopic ellipsometry to track the Ge content and the other energy-independent dielectric function parameters as functions of depth as described here provides a unique opportunity for optimization of compositionally graded structures in solar cell devices.

Acknowledgment

This research is supported by NREL TFPPP Subcontract No. ZXL-5-44205-06.

References

[1] X. Deng and E.A. Schiff, in: *Handbook of Photovoltaic Science and Engineering*, edited by A. Luque and S. Hegedus (Wiley, New York, 2003), p. 505.

[2] B.E. Pieters, M. Zeman, R.A.C.M.M. van Swaaij, and W.J. Metselaar, *Thin Solid Films* **451-452**, 294 (2004).

[3] A.S. Ferlauto, G.M. Ferreira, J.M. Pearce, C.R. Wronski, R.W. Collins, X. Deng, and G. Ganguly, *J. Appl. Phys.* **92**, 2424 (2002).

[4] G.E. Jellison, Jr., and F.A. Modine, *Appl. Phys. Lett.* **69**, 371 (1996); **69**, 2137 (1996).

[5] H. Fujiwara, J. Koh, C.R. Wronski, and R.W. Collins, *Appl. Phys. Lett.* **70**, 2150 (1997).

[6] N.J. Podraza, C.R. Wronski, M.W. Horn, and R.W. Collins, *Mater. Res. Soc. Symp. Proc.* **910**, A.10.1.1-6 (2006).

Section 3

ZnO film thickness study for Ag/ZnO back reflector

Xiesen Yang, Dinish Attygalle, Xianbo Liao, Xunming Deng
Department of Physics and Astronomy, University of Toledo, Toledo, OH 43606, USA

1. Introduction

ZnO film as a buffer layer between the metal back reflector (BR) and the amorphous or nano-crystalline silicon layers is a standard structure in thin film silicon solar cells. It is desirable to have certain thickness to prevent the inter-diffusion of metal and silicon. It may need even thicker ZnO layer to fully cover the metal surface when the metal layer is highly textured. But the thicker ZnO layer may absorb much light and cause extra optical loss. This work is trying to answer this question.

2. Experimental details

In this study, an intrinsic ZnO ceramic target was used. ZnO film sample was deposited on Corning glass 1737 by RF sputtering with about 2300nm thickness. Then transmission of this sample was measured. From transmission data, the film thickness and refractive index was calculated, also the absorption coefficients α (cm^{-1}) as a function of wavelength by the method of R Swanepoel [1]. Having the absorption coefficients, the film absorption spectrum at different thickness was calculated at the interest wavelength range (600 ~ 1200 nm). The integrated absorption in percentage at this range was calculated also.

A series of complete Ag/ZnO BRs were fabricated. Ag layer condition was fixed at 300 ºC and 350 nm; ZnO layers were deposited at 150 ºC and different thickness: 2300, 1500, 700, and 350 nm. Then these BRs were evaluated by nc-Si solar cells deposited on glass substrate [2]. The nc-Si cells with glass/ITO/n/i/p/ITO structure were directly deposited on Teck15 glass without BR. The BR sample was put underneath the glass to function as external BR for the cells. Then short circuit current density J_{sc} of these cells was taken to evaluate the BR samples.

3. Results and discussion

3-1). The ZnO film absorption evaluation.

Figure 1 shows the transmission data of the 2300 nm thick intrinsic ZnO film sample. It has high transmission in a wide range. From the data, the absorption coefficients were deduced. And then the absorption spectrum (A) at different thickness 2300, 1500, 700, and 350 nm was calculated at the interest wavelength range (600 ~ 1200 nm). The integrated absorption over

AM1.5 spectrum at this range was calculated for 2300, 1500, 700, and 350 nm to be 2.54%, 1.68%, 0.79%, 0.40% respectively. Fig. 2. shows 1-A of the above calculations

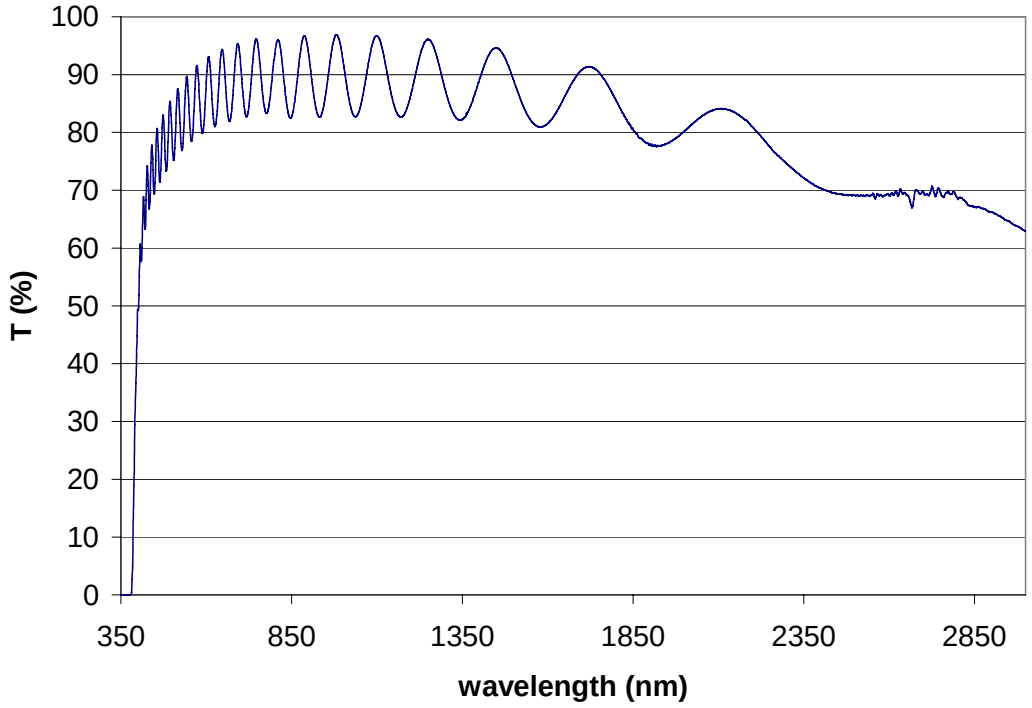

Fig.1 Transmittance of ZnO film.

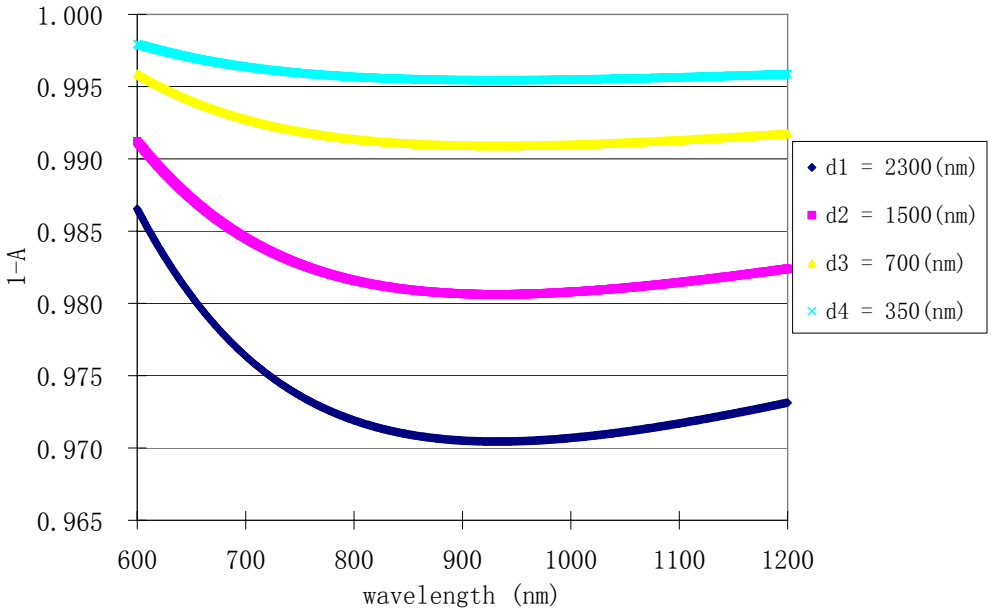

Fig. 2 The calculated 1-Absorption (1-A) at different thickness of ZnO film.

3-2). The simplified measurement of BR by nc-Si solar cells on glass

The complete Ag/ZnO BRs were evaluated by nc-Si solar cells deposited on Tech15 glass. The J_{sc} was taken to indicate the BR effect. Fig.3 shows the average J_{sc} of the cells. It shows that the thicker ZnO leads to lower J_{sc}. This trend is consistent with the previous analysis film absorption. The current difference of the sample with 350 nm and 1500nm ZnO is about 4%, compared with the film absorption 0.4% and 1.68%. The sample without ZnO film has the highest current, maybe due to the non absorption of ZnO film and the Ag/ZnO interface-caused absorption.

But there is air gap between the glass substrate and BR in this method. This is not the case in real device. This air gap introduces tow interfaces which may cause extra optical loss and may enlarge the effect of ZnO film absorption loss.

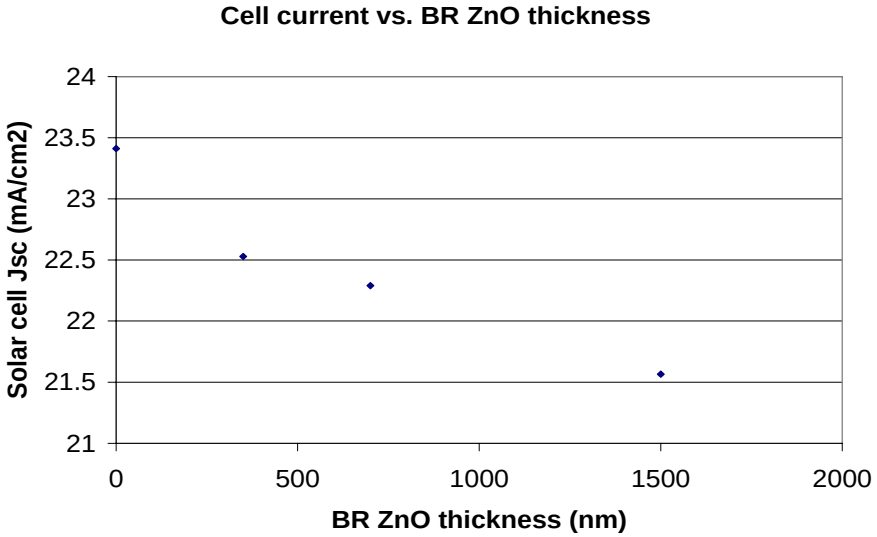

Fig. 3 Test nc-Si cell J_{sc} on top of BR sample with different ZnO layer thickness.

4. Conclusion

The intrinsic ZnO film has very good transmittance. The integrated optical absorption loss on solar spectrum over range 600 ~ 1200 nm is only about 2.54% with a thickness about 2300 nm. When the complete Ag/ZnO BRs are evaluated by nc-Si cells on glass, it shows that the thicker ZnO leads to smaller J_{sc}. But this method needs further analysis since there is an air gap which may cause extra optical loss during measuring.

5. References

[1] R Swanepoel, *J. Phys. E: Sci. Instrum*, Vol. **16**. 1983.
[2] S. Hegedus and X. Deng, *Twenty Fifth IEEE Photovoltaic Specialists Conference*--1996, p.1061 (1996).

Section 4

Optical Simulations of the Effects of Ag/ZnO Interlayer at the Back-Reflector for Thin Film a-Si:H Solar Cells

A. Parikh, D. Sainju, M. Syed,[#] N. J. Podraza, and R. W. Collins

Department of Physics and Astronomy, the University of Toledo, Toledo, OH 43606, USA
Dept. of Physics & Optical Engineering, Rose-Hulman Institute of Technology, Terre Haute, IN 47803, USA

1. Introduction

Polarization analysis of specular and textured thin film amorphous silicon (a-Si:H) based solar cell structures, applying spectroscopic ellipsometry (SE) measurements, demonstrates that microscopic surface and interface roughness is ubiquitous and exerts considerable influence on the specular reflectance and hence the quantum efficiency of the solar cells [1,2]. Microscopic roughness in this context is defined as surface/interface modulations with in-plane correlation lengths at least an order of magnitude smaller than the center wavelength λ_c of the analysis light beam. For a-Si:H based solar cells, λ_c is approximately 500 nm for the wavelength range of interest. The optical effect of microscopic surface and interface roughness can be simulated by inserting a layer at the interface between two adjacent media. The optical thickness of this interface layer scales with the root mean square (rms) roughness value, e.g., as would be deduced from probe microscopy, and its optical properties are determined from the Bruggeman effective medium approximation, assuming a composite of the overlying and underlying materials [3].

In addition to surface and interface roughness, chemically and optically modified interface regions can occur in the solar cell structures, and these can have a significant influence on the reflectance, absorbance, and quantum efficiency. Very little research has been performed to assess the nature of such layers and their impact on solar cell performance. Over the last quarter, simulations of the optical quantum efficiency (QE) of a-Si:H based solar cells in the substrate/BR/n-i-p configuration have explored the effects of a modified Ag/ZnO interface layer in the Ag/ZnO back reflector. This interface layer is significant because of the absorption losses that it generates upon reflection of near-infrared wavelengths back into the cell. Although introducing macroscopic roughness in addition to the microscopic roughness at the Ag/ZnO interface leads to scattering of the near-infrared light upon back-reflection, thereby increasing the optical path length and hence the QE, this roughness also has an offsetting detrimental effect in that it enhances absorption losses at the Ag/ZnO interface. (Note that macroscopic roughness in this context is defined as surface/interface modulations with in-plane correlation lengths larger than the microscopic scale but smaller than the lateral coherence length of the light at $\lambda=\lambda_c$.)

2. Experimental Details

A silver film with a microscopic surface roughness layer thickness of 28 Å (as deduced by real time SE at the end of the deposition) was deposited by magnetron sputtering onto a c-Si wafer substrate covered with a native oxide layer (d_{ox} ~ 15 Å). This Ag film was deposited at a nominal substrate temperature of T=50°C, a gas pressure of ~ 4 mTorr, an argon gas flow of 10 sccm, and a target power of P=50 W. By increasing the substrate temperature to T~170°C, a much larger microscopic roughness layer thickness of d_s = 105 Å is obtained by the end of Ag deposition. ZnO is deposited at room temperature on both Ag surfaces using the same sputtering conditions as for the Ag.

Ellipsometric analyses of Ag growth and Ag/ZnO interface formation are performed using a rotating-compensator multichannel instrument that can provide spectra (0.75 to 6.5 eV) in (ψ, Δ) with minimum acquisition time of 32 ms as an average over a single pair of optical cycles. Pairs of (ψ, Δ) spectra were collected within a time of ~1 s, as averages over ~30 optical cycle pairs in order to improve precision. During the acquisition time for one set of (ψ, Δ) spectra, a bulk layer thickness of ~ 6 Å accumulates at the maximum deposition rates used here. Analyses of all spectra involve numerical inversion and least-squares regression algorithms. The angle of incidence was 64.88 ± 0.09°.

3. Model Inputs

Figure 1 summarizes the basic optical model used for computing the characteristics of the a-Si:H triple junction solar cell. The thicknesses of the i-layers in Figure 1 are chosen for current matching in the triple junction device with a current density of 7.3 mA/cm^2 under a global air mass 1.5 solar spectrum. The model used here is based on normal-incidence specular reflection and transmission at interfaces using standard Fresnel coefficients, and the multiply-reflected beams within all solar cell layers are assumed to add coherently. It should be noted that non-specular scattering -- which is an important aspect of light trapping -- has yet to be incorporated into the modeling procedure due to the present lack of experimentally-verifiable inputs. Three different Ag/ZnO back-reflector structures were modeled: i) a structure with an initial Ag surface roughness of d_s = 28 Å prepared at University of Toledo (UT), ii) a structure with d_s = 105 Å also prepared at UT, and iii) a structure prepared at Energy Conversion Devices (ECD) used as a standard. The back-reflector structures with higher initial Ag surface roughness (including the UT sample with d_s = 105 Å and most likely the ECD back-reflector as well) have revealed significantly different interface layer dielectric functions compared to the sample with lower initial roughness (d_s = 28 Å), as shown in Figure 2. The interface layer dielectric functions for all three structures were obtained using Kramers-Kronig consistent parameterized models.

laminate	--
ITO	750 Å
p-layer	100 Å
i-layer (1.8 eV)	930 Å
n-layer	100 Å
p-layer	100 Å
i-layer (1.6 eV)	2300 Å
n-layer	100 Å
p-layer	100 Å
i-layer (1.4 eV)	2100 Å
n-layer	100 Å
ZnO	2000 Å
interface layer	0 – 400 Å
Ag	1500 Å
stainless steel	--

Fig. 1: Schematic multilayer optical structure of a triple-junction a-Si:H based solar cell in the substrate/BR/n-i-p configuration. The intent of such modeling is to assess the role of the interface layer between the Ag and ZnO. Other non-idealities throughout the structure, including microscopic surface and interface roughness layers, are neglected.

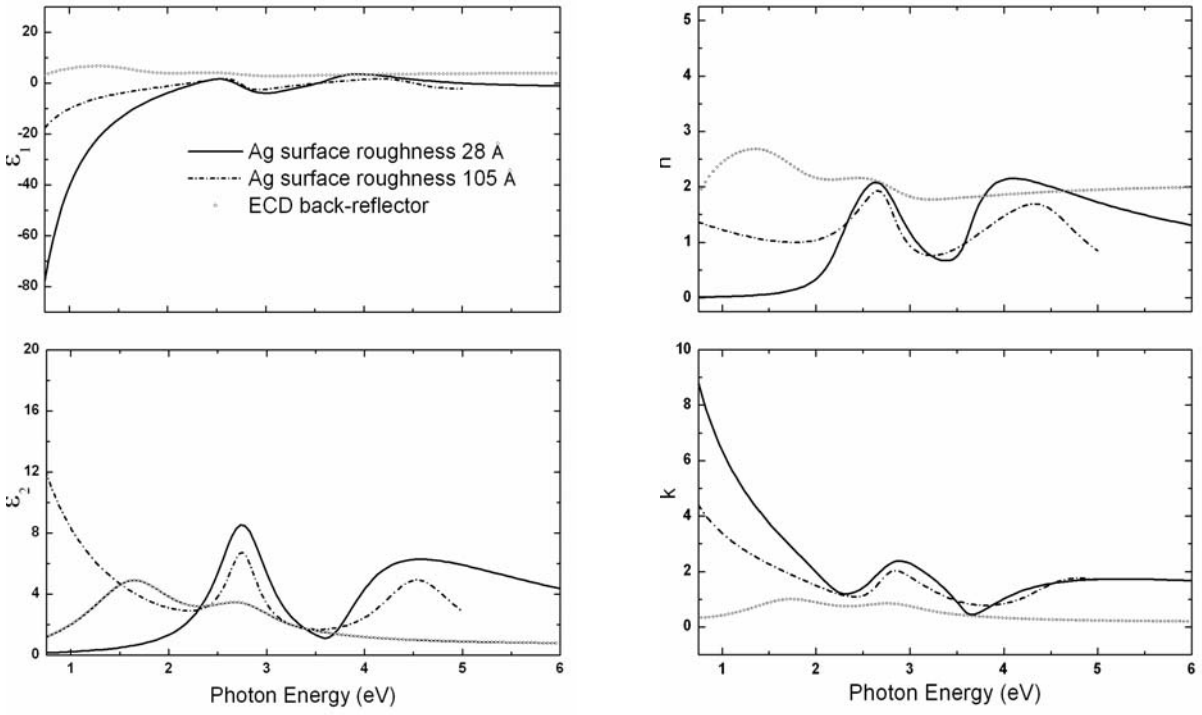

Fig. 2: Real and imaginary parts of the dielectric functions of the Ag/ZnO interface layers for samples prepared with different initial Ag surface roughness conditions. These results were obtained in best fits to real time (UT: d_s = 28 and 105 Å) or ex situ (ECD) spectroscopic ellipsometry data.

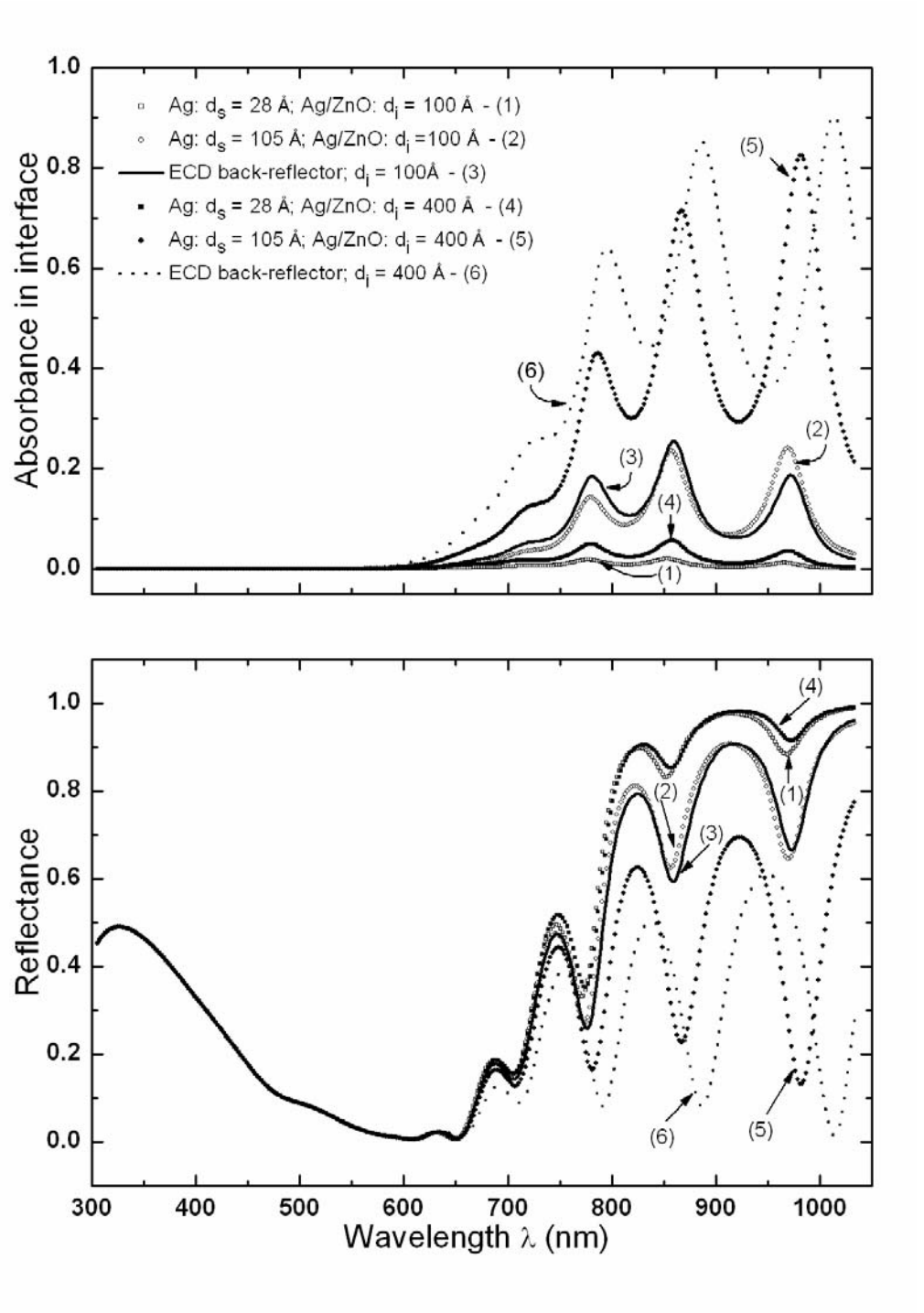

Fig. 3: Predicted spectra in the absorbance (upper panel) within the Ag/ZnO interface layer of the structure of Fig. 1, using different dielectric functions for the interface layer as shown in Fig. 2; also shown are the corresponding predicted reflectance spectra (lower panel) for the entire solar cell multilayer structure. The three different interface dielectric functions were modeled each with two different interface layer thicknesses as shown.

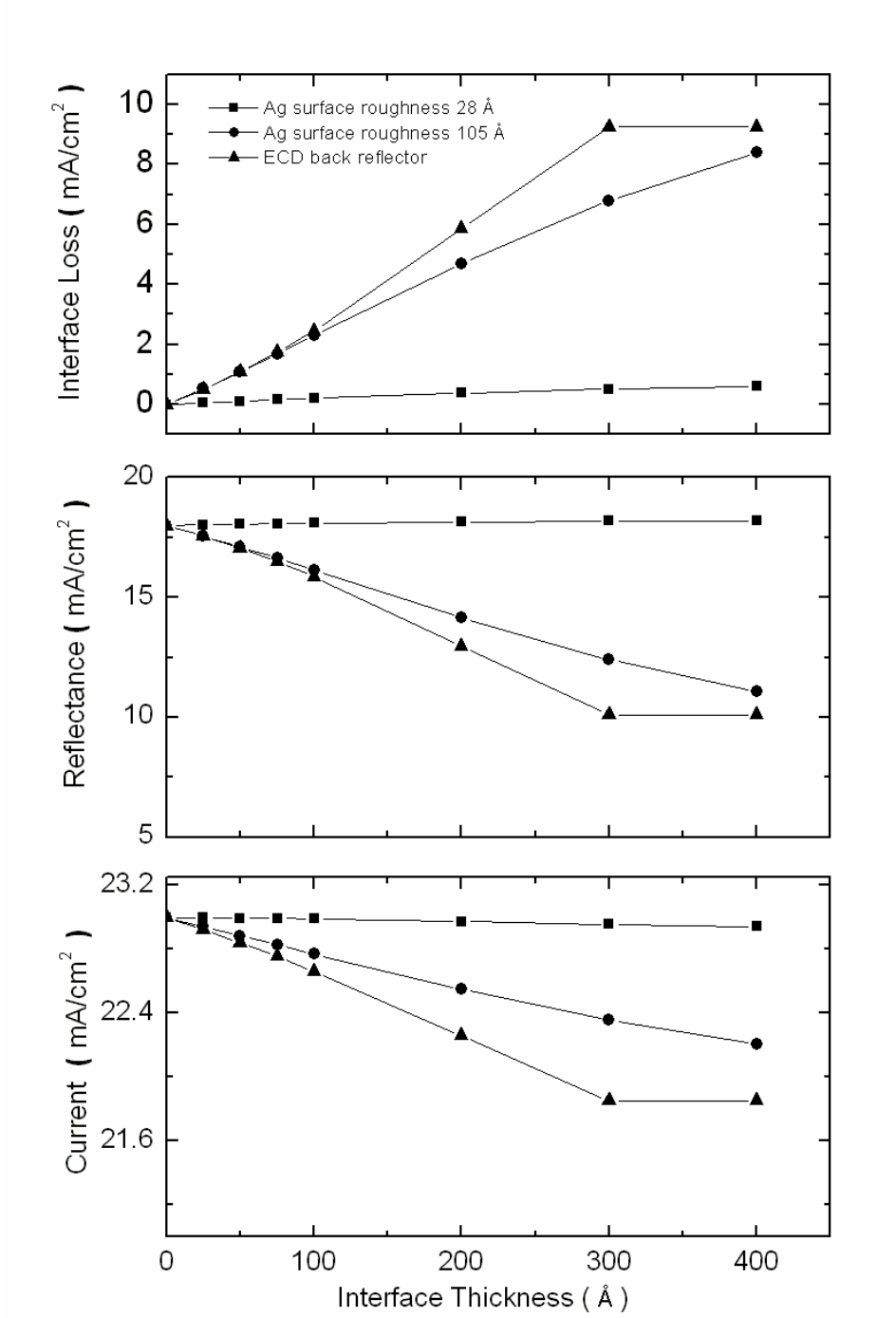

Fig. 4: a) Interface loss by absorption, b) reflectance which is available for collection in improved back-reflector designs, and c) current generated by absorption in the three i-layers, assuming that all electron hole pairs contribute to the current. These results are plotted as functions of interface layer thickness for each type of interface layer dielectric function extracted from the ellipsometric studies.

4. Results and Discussion

The upper panel of Figure 3 shows the predicted optical absorbance within the three different Ag/ZnO interface layers for the solar cell structure of Fig. 1. The plot compares interface thicknesses of 100 Å and 400 Å for each one of the three interface dielectric functions of Fig. 2. The onset of absorption in all cases occurs at a wavelength of ~ 600 nm, showing that all incident irradiance below that wavelength is absorbed by the overlying structure. Enhanced absorption with increasing wavelengths above 600 nm can be attributed to the fact that increased irradiance reaches the back-reflector interface. The model predicts significant absorption in the interface layer of the ECD and UT d_s=105 Å back-reflectors in the spectral region of 700-1000 nm for both interface thicknesses. The model incorporating initial Ag surface roughness of d_s = 28 Å shows minor interlayer absorption losses and thus strong reflected irradiance (lower panel of Fig. 3) that potentially could be collected with proper back-reflector design incorporating light trapping.

The key point of the results of Fig. 3 is that an increase in the initial Ag surface roughness increases the absorption loss through the interface. Accordingly, there is less reflected irradiance available for capture in a second pass (or more) through the cell. In particular, the ECD back-reflector which incorporates macroscopic roughness as well as microscopic roughness leads to the largest absorbance, presumably due to the largest initial roughness on the Ag. The similarity of the results for the UT d_s=105 Å and the ECD back-reflector structures suggests that the former structure also incorporates macroscopic roughness. This can be assessed by comparing the measured reflectance with that predicted from complete polarization analysis of the multilayer structure (which is not influenced by scattering losses from the specular beam). The difference is due to non-specular scattering attributed to macroscopic roughness which can be quantified in a separate modeling procedure. This analysis and the associated modeling is in progress.

Figure 4(a) shows the potential gain in J_{sc} that could be achieved if *all absorbance losses* in the ZnO/Ag interface could be eliminated and converted to useful current through absorption in the i-layers in one or more passes through the solar cell. This current gain is obtained by integrating the product of the optical absorbance and the AM 1.5 spectral photon flux over the spectral range from 305 to 1033 nm. The interface absorbance is predicted to strongly affect the performance of the ECD back-reflector, but does not significantly impact the model with an interface dielectric function based on initial Ag surface roughness of d_s = 28 Å. In particular, it can be seen that for low initial Ag surface roughness, the cell performance does not depend strongly on the interface thickness. Figure 4(c) shows the summed integrated current from all three active layers over the same spectral range. In general, this summed current is predicted to decrease with increasing interface thickness. The change in this current is attributed to the change in quantum efficiency of the bottom i-layer with the lowest band gap of E_g = 1.4 eV. This means that infrared photons not absorbed in interface layer and thus reflected back from the Ag are absorbed in the lowest band gap active layer. The current through the highest bandgap active layer, E_g = 1.8 eV, remains nearly unchanged with interface layer thickness, while the middle band gap active layer, E_g = 1.6 eV, exhibits only minor variations. Such behavior is to be expected since the role of the back-reflector is to enhance absorbance in the bottom cell**.** Thus, any loss by absorption in the interface layer leads to a loss in potential current generated by the bottom i-layer.

5. Summary

Optical simulations have been performed to investigate the effect of Ag/ZnO interface layers in back-reflectors for thin film triple junction a-Si:H solar cells in the n-i-p configuration. The role of interface layers generated by differing amounts of initial Ag surface roughness has been explored. It has been observed that increasing the initial surface roughness of Ag increases the losses through absorption in the interlayer. As expected, increasing the interface thickness for a given interface layer dielectric function enhances the absorption losses in the interlayer. The goal of the back-reflector fabrication studies is to identify the origins of the interface losses and eliminate them through modifications in the back-reflector design. Modeling studies such as these supplement the experimental work and predict the improvements that may be expected.

Acknowledgment

This research is supported by NREL TFPPP Subcontract No. ZXL-5-44205-06.

References

[1] R. W. Collins, J. Koh, H. Fujiwara, P. I. Rovira, A. S. Ferlauto, J. A. Zapien, C.R.Wronski and R.Messier, *App. Surf. Sci.* **154**, 217 (2000).

[2] B. Drevillon, *Prog. Cryst. Growth Charact. Mater.* **27**, 1 (1993).

[3] H. Fujiwara, J. Koh, P. I. Rovira, and R. W. Collins, *Phys. Rev. B* **61**, 10832 (2000).